

Self-Consistent Orthogonalized-Plane-Wave and Empirically Refined Orthogonalized-Plane-Wave Energy-Band Models for Cubic ZnS, ZnSe, CdS, and CdSe

D. J. STUKEL,* R. N. EUWEMA, AND T. C. COLLINS

Aerospace Research Laboratories, Wright-Patterson Air Force Base, Ohio 45433

AND

F. HERMAN AND R. L. KORTUM†

Lockheed Palo Alto Research Laboratory, Palo Alto, California 94304

(Received 23 October 1968)

First-principles orthogonalized-plane-wave energy-band calculations have been carried out for cubic ZnS, ZnSe, CdS, and CdSe, using a nonrelativistic formalism and Slater's free-electron exchange approximation. The calculations were first carried out in terms of a physically realistic trial crystal potential, and then iterated to obtain a self-consistent solution. So far as we are aware, these are the first fully convergent, fully self-consistent energy-band solutions reported for cubic II-VI semiconducting compounds. In spite of the simplified treatment of exchange effects, and the neglect of relativistic and correlation effects, the first-principles solutions are in qualitative and semi-quantitative agreement with experiment in all cases. It is shown briefly how improved solutions can be obtained by introducing small, carefully chosen empirical corrections. The adequacy of various energy-band models was tested by calculating the optical spectrum (actually ϵ_2) and comparing this with the experimental spectrum. Actually, this comparison checks only certain features of these energy-band models. It would be helpful to have additional experimental information so that other features, such as the energy separation between principal and subsidiary conduction-band minima, could also be checked.

I. INTRODUCTION

DURING the past few years, a great deal of experimental and theoretical effort has been devoted to the study of the energy-band structure and related properties of II-VI compounds.¹ The band structure of these compounds has been calculated by a variety of methods, including the empirical pseudopotential method,²⁻⁴ the empirically refined Korringa-Kohn-Rostoker (ER-KKR) method,⁵⁻⁷ the empirically refined orthogonalized-plane-wave (ER-OPW) method,⁸⁻¹⁰

and the first-principles self-consistent OPW (SC-OPW) method.^{11,12}

All of these approaches, whether purely empirical, semiempirical, or purely first-principles in character, lead to energy-band pictures which are in substantial qualitative agreement with one another. However, different theoretical treatments lead to quantitative predictions which may differ from one another by a few to several tenths of an eV (or more). Of course, some of these predictions—such as the direct band gap—can be checked against experiment, while others—such as the energy separation between principal and subsidiary conduction-band minima—cannot be checked with any degree of accuracy by analysis of *available* experimental information. Although we already know a great deal about the band structure of II-VI compounds, there is still a pressing need for more incisive theoretical (and experimental) treatments.

Since the first study of (hexagonal) ZnS by the OPW method in 1960,¹³ there has been a steady improvement in OPW band calculations. In large measure, this improvement has been made possible by the increasing availability of faster and higher-capacity electronic digital computers. While it would have been prohibitively difficult in 1960 to carry out self-consistent OPW energy-band calculations using variational wave functions consisting of 200 or more OPWs, such cal-

* Part of this work has been submitted by D. J. Stukel to the Air Force Institute of Technology, Air University, in partial fulfillment of the requirements for the degree of Doctor of Science.

† The Lockheed contribution to this paper was sponsored by the Lockheed Independent Research Fund; the Air Force Cambridge Research Laboratories, Office of Aerospace Research, under Contract No. AF19(628)-5750; and the Aerospace Research Laboratories, Office of Aerospace Research, under Contract No. AF33 (615)-5072.

¹ *II-VI Semiconducting Compounds, 1967 International Conference*, edited by D. G. Thomas (W. A. Benjamin, Inc., New York, 1967).

² M. L. Cohen and T. K. Bergstresser, *Phys. Rev.* **141**, 789 (1966).

³ T. K. Bergstresser and M. L. Cohen, *Phys. Rev.* **164**, 1069 (1967).

⁴ M. L. Cohen, in Ref. 1, p. 462.

⁵ P. Eckelt, doctoral dissertation, University of Marburg, 1967 (unpublished).

⁶ P. Eckelt, O. Madelung, and J. Treusch, *Phys. Rev. Letters* **18**, 656 (1967).

⁷ J. Treusch, P. Eckelt, and O. Madelung, in Ref. 1, p. 588.

⁸ J. L. Shay, W. E. Spicer, and F. Jernan, *Phys. Rev. Letters* **649** (1967).

⁹ F. Herman, R. L. Kortum, C. D. Kuglin, and J. L. Shay, in Ref. 1, p. 503.

¹⁰ F. Herman, R. L. Kortum, C. D. Kuglin, and J. P. Van Dyke, in *Methods in Computational Physics*, edited by B. Alder, S. Fernbach, and M. Rotenberg (Academic Press Inc., New York, 1968), Vol. 8, Chap. 6.

¹¹ R. N. Euwema, T. C. Collins, D. G. Shankland, and J. S. DeWitt, *Phys. Rev.* **162**, 710 (1967). See also T. C. Collins, R. N. Euwema, and J. S. DeWitt, in Ref. 1, p. 598.

¹² T. C. Collins, D. J. Stukel, and R. N. Euwema, *Bull. Am. Phys. Soc.* **13**, 412 (1968), Abstract CJ3.

¹³ F. Herman and S. Skillman, in *Proceedings of the International Conference on Semiconductor Physics, Prague, 1960* (Publishing House of Czechoslovak Academy of Sciences, Prague, 1961), p. 20.

culations are now being performed on a routine basis at both of our laboratories.

Energy-band results for a variety of II-VI compounds, based on preliminary ER-OPW and SC-OPW band calculations, have been reported in a number of recent papers.⁸⁻¹² Continuing improvements in our computational techniques have enabled us to carry out still better ER-OPW and SC-OPW band calculations. In the present paper we will report jointly our most recent ER-OPW and SC-OPW solutions for cubic ZnS, ZnSe, CdS, and CdSe. The purposes of this paper are the following:

- (1) To report for the first time the outcome of highly convergent, highly self-consistent OPW band calculations for four representative sphalerite-type crystals (ZnS, ZnSe, CdS, CdSe).
- (2) To compare the results of non-self-consistent and self-consistent OPW (NSC-OPW and SC-OPW) band calculations.
- (3) To compare our results with experiment and with other theoretical results.
- (4) To assess the physical realism of the present set of SC-OPW band calculations.
- (5) To suggest further improvements in such calculations.

II. SELF-CONSISTENT OPW BAND CALCULATIONS

The technique of carrying out nonrelativistic self-consistent OPW band calculations was outlined by Herman in 1964.¹⁴ The present approach is quite similar to that discussed in Ref. 14, though there are some differences in the details.¹⁵ In brief, one constructs a trial crystal potential and then determines the energy levels and electronic wave functions of the core states and of a representative sample of the valence states. An improved crystal potential is then constructed in terms of these wave functions, and the process is repeated until successive iterations yield substantially the same crystal potential. In practice, the iterative process is continued until corresponding Fourier coefficients of crystal potential change by less than 0.0005 Ry in successive iterations. When this stage is reached, the energy-band scheme is usually stable to within about 0.02 eV. For our purposes, this constitutes a self-consistent energy-band calculation.

The starting crystal potential is represented by a spatial superposition of nonrelativistic self-consistent atomic potentials, in the manner of Herman and Skillman.¹³ This crystal-potential model, which is sometimes called the *overlapping atomic potential model*, also forms

¹⁴ F. Herman, in *Proceedings of the International Conference on the Physics of Semiconductors, Paris, 1964* (Dunod Cie., Paris, 1964), p. 3.

¹⁵ R. N. Euwema, D. J. Stukel, and T. C. Collins (to be published). This paper will contain a more complete account of the present set of SC-OPW band calculations.

TABLE I. Relativistic mass-velocity and Darwin corrections for selected interband transitions. These estimates were obtained from NSC-OPW band calculations by first-order perturbation theory. All entries are in eV.

Transition Energy	ZnS	ZnSe	CdS	CdSe
$\Gamma_{15c}-\Gamma_{15v}$	0.0	0.2	-0.2	0.0
$\Gamma_{1c}-\Gamma_{15v}$	-0.3	-0.6	-0.5	-0.8
$X_{3c}-\Gamma_{15v}$	-0.2	0.0	-0.6	-0.3
$X_{1c}-\Gamma_{15v}$	0.0	0.1	-0.1	0.1
$X_{5v}-\Gamma_{15v}$	0.0	0.1	0.0	0.0
$L_{3c}-\Gamma_{15v}$	0.0	0.2	-0.1	0.1
$L_{1c}-\Gamma_{15v}$	-0.3	-0.3	-0.6	-0.5
$L_{3v}-\Gamma_{15v}$	0.0	0.0	0.0	0.0

the basis of non-self-consistent OPW (NSC-OPW) band calculations.¹⁶⁻¹⁸

All of the calculations reported in this paper are based on a nonrelativistic crystal Hamiltonian and on Slater's free-electron exchange approximation.¹⁹ We have repeated most of these calculations using the Kohn-Sham version²⁰ of this approximation. Although both of these exchange approximations lead to valence and conduction band structures which are quite similar from a qualitative point of view, the Kohn-Sham version usually leads to smaller energy separations between the valence and conduction bands. The reductions in forbidden bandwidth range from a few to several tenths of an eV. Since there is usually closer quantitative agreement between theoretical and experimental interband energies for the Slater-type solutions, we will focus our attention on these in what follows, and not discuss the Kohn-Sham solutions further at this time.

The neglect of relativistic and spin-orbit coupling effects can lead to significant errors in the calculated band structure, particularly in crystals composed of the heavier atoms, such as CdSe. The spin-orbit splitting can be estimated and taken into account in a variety of ways.^{10,11,21,22} Rough estimates of the relativistic (mass-velocity and Darwin) corrections²³ can be obtained by applying first-order perturbation theory to SC-OPW (or NSC-OPW) solutions¹⁶; such estimates are listed in Table I. Even allowing for the fact that such estimates are accurate to only about 20%, it is clear that the neglect of relativistic effects can lead to errors in interband energy separations of a few to several tenths

¹⁶ F. Herman, R. L. Kortum, C. D. Kuglin, and R. A. Short, in *Quantum Theory of Atoms, Molecules, and the Solid State*, edited by P. O. Löwdin (Academic Press Inc. New York, 1966), p. 381.

¹⁷ F. Herman, R. L. Kortum, and C. D. Kuglin, *Intern. J. Quan. Chem.* **15**, 533 (1967).

¹⁸ F. Herman, R. L. Kortum, C. D. Kuglin, and J. P. Van Dyke, in *Energy Bands in Metals and Alloys*, edited by J. T. Waber and L. H. Bennett (Gordon and Breach, Science Publishers, Inc., New York, 1968), p. 19.

¹⁹ J. C. Slater, *Phys. Rev.* **81**, 385 (1951).

²⁰ W. Kohn and L. J. Sham, *Phys. Rev.* **140**, A1133 (1965).

²¹ S. Bloom and T. K. Bergstresser, *Solid State Commun.* **6**, 465 (1968).

²² P. Eckelt, *Solid State Commun.* **6**, 489 (1968).

²³ F. Herman, C. D. Kuglin, K. F. Cuff, and R. L. Kortum, *Phys. Rev. Letters* **11**, 541 (1963).

of an eV. The most significant errors will normally be associated with energy separations between *s*-like conduction-band states and *p*-like valence-band states. The direct band gap ($\Gamma_{1c} - \Gamma_{15v}$) is an example of such an energy separation. It appears that the inclusion of relativistic effects tends to reduce the energy separation between valence- and conduction-band states in sphalerite-type crystals.

In order to take relativistic and spin-orbit coupling effects into account properly, it is necessary to work within the framework of a fully relativistic crystal Hamiltonian.^{10,24,25} Although fully relativistic OPW band calculations based on a trial crystal potential have already been carried out for over 25 different crystals, including several II-VI compounds,¹⁰ we have not yet attempted to iterate the solutions so as to achieve self-consistency. For the present, we must content ourselves with comparisons of nonrelativistic (NREL) solutions, i.e., NREL-NSC-OPW versus NREL-SC-OPW. In due course, we hope to be able to make similar comparisons between REL-NSC-OPW and REL-SC-OPW solutions, where REL denotes relativistic. In any event, we would expect the future comparison of relativistic solutions to have a great deal in common with the present comparison of nonrelativistic solutions.

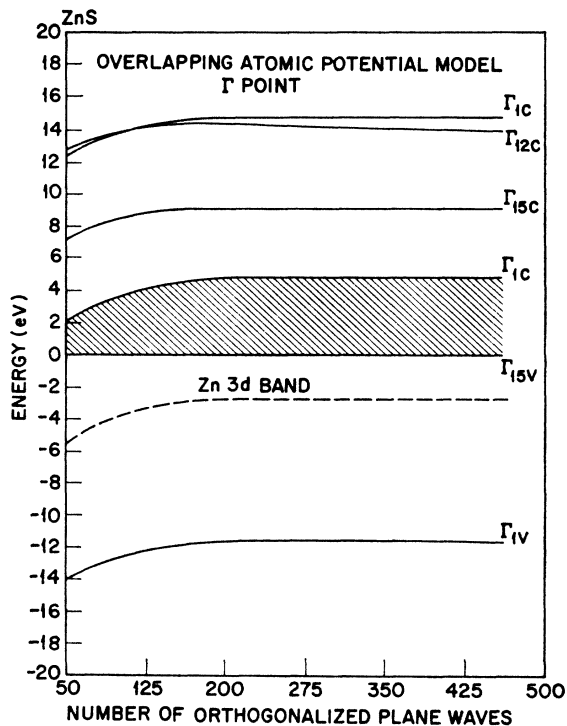


Fig. 1. Convergence study of NSC-OPW energy levels at Γ point in cubic ZnS. The location of 3*d* Zn level is also shown.

²⁴ P. Soven, Phys. Rev. 137, A1706 (1965).

²⁵ F. Herman, R. L. Kortum, I. B. Ortenberger, and J. P. Van Dyke, J. Phys. (Paris) (to be published).

In the present calculations, we wish to achieve the highest practical degree of mathematical accuracy. In all types of OPW band calculations, it is important to make sure that enough OPW terms are included in the variational wave functions to insure a high degree of convergence. The convergence properties of NSC-OPW band calculations for cubic ZnS are illustrated in Fig. 1. In this drawing, the energy levels at Γ are shown as a function of the number of OPWs used. In order to obtain solutions that are convergent to about 0.1 eV, it is necessary to use about 181 OPWs. If one increases the number of OPWs from 181 to 229, Γ_{1c} and Γ_{1v} change by about 0.01 eV, Γ_{15c} changes by about 0.05 eV, and Γ_{15v} changes by about 0.09 eV. Further increases in the number of OPWs lead to negligible changes in these

TABLE II. Zonal weighting factors used in integrating over the volume of the Brillouin zone. The first set involves only the Γ point; the second set only *L*; the third set Γ , *X*, and *L*; and the fourth set Γ , *X*, *L*, and *W*.

Point	Γ	<i>L</i>	Γ - <i>X</i> - <i>L</i>	Γ - <i>X</i> - <i>L</i> - <i>W</i>
Γ	1.0	0.0	0.125	0.1258
<i>X</i>	0.0	1.0	0.375	0.1731
<i>L</i>	0.0	0.0	0.5	0.3600
<i>W</i>	0.0	0.0	0.0	0.3411

TABLE III. Comparison of ZnSe SC-OPW energy levels at Γ and *L* points, obtained on the basis of four different zone-sampling schemes (229 OPWs). All entries are in eV.

Level	Γ	<i>L</i>	Γ - <i>X</i> - <i>L</i>	Γ - <i>X</i> - <i>L</i> - <i>W</i>
Γ_{15c}	4.64	6.43	6.42	6.66
Γ_{1c}	1.65	2.75	2.75	2.94
Γ_{15v}	0.0	0.0	0.0	0.0
Γ_{1v}	-11.86	-11.83	-11.82	-11.82
<i>L</i> _{1c}	9.65	9.57	9.69	9.72
<i>L</i> _{3c}	5.62	7.11	7.10	7.32
<i>L</i> _{1c}	2.08	3.59	3.57	3.79
<i>L</i> _{3v}	-0.91	-0.66	-0.66	-0.64
<i>L</i> _{1v}	-5.72	-4.53	-4.54	-4.40
<i>L</i> _{1v}	-10.46	-10.81	-10.80	-10.84

energy levels. The convergence properties of the energy levels at other points in the zone are similar to those shown in Fig. 1.

In determining the valence electron charge distribution in SC-OPW band calculations, one sums the contributions of all occupied valence band states—in principle. In practice, one performs this sum by using a representative sample of points in the reduced zone, and assigning suitable weights to the various points. In such calculations, it is also necessary to check the convergence of the solutions as a function of the number of points sampled in the reduced zone.

In Table II we show the weights used in four successively finer samples, and in Table III we show the corresponding self-consistent energy levels at Γ and *L* for cubic ZnSe (using 229 OPWs at Γ and a comparable number of OPWs at the other sample points). The

weights for the first three types of samples hardly need explanation. The weights for the final four-point sample are proportional to those fractions of the reduced zone which lie closer to the points in question than to the remaining points.

It is clear from Table III that the sample involving only the zone center is not representative of the zone as a whole. The sample involving only the L point is decidedly better. In fact, one obtains nearly the same energy band structure using L alone or the combination of Γ , X , and L . The inclusion of the zone corners (W) leads to changes in the band structure of the order of 0.1 to 0.2 eV. According to our best estimates, the four-

TABLE IV. SC-OPW energy eigenvalues for cubic ZnS, ZnSe, CdS, and CdSe, based on four-point (Γ, X, L, W) zone sampling. 229 OPWs were used at Γ , and a comparable number of OPWs at X , L , and W . The zero of energy has been placed at the top of the valence band (Γ_{15v}). All entries are in eV.

Level	ZnS	ZnSe	CdS	CdSe
Γ_{15c}	7.99	6.66	7.58	6.61
Γ_{1c}	3.77	2.94	2.72	2.32
Γ_{15v}	0.00	0.00	0.00	0.00
Γ_{1v}	-11.77	-11.82	-10.92	-10.92
X_{3c}	5.95	4.49	5.68	4.76
X_{1c}	5.01	4.19	4.89	4.21
X_{5v}	-1.61	-1.65	-1.44	-1.36
X_{3v}	-3.93	-4.31	-3.33	-3.46
X_{1v}	-10.29	-10.48	-9.72	-9.97
$X_{3c}-X_{5v}$	7.55	6.15	7.12	6.13
$X_{1c}-X_{5v}$	6.62	5.84	6.33	5.58
L_{1c}	9.88	9.72	8.46	8.44
L_{3c}	8.62	7.31	8.24	7.20
L_{1c}	4.96	3.79	4.30	3.67
L_{3v}	-0.61	-0.64	-0.56	-0.53
L_{1v}	-4.20	-4.40	-3.62	-3.57
L_{1v}	-10.66	-10.84	-10.00	-10.21
$L_{3c}-L_{3v}$	9.23	7.96	8.80	7.73
$L_{1c}-L_{3v}$	5.57	4.42	4.86	4.20
W_{1c}	7.47	6.38	6.59	6.02
W_{3c}	7.06	6.44	6.66	6.09
W_{3v}	-1.96	-1.98	-1.72	-1.60
W_{2v}	-2.10	-2.28	-1.74	-1.79
W_{1v}	-3.70	-4.04	-3.19	-3.26
W_{4v}	-10.26	-10.46	-9.68	-9.92
$W_{3c}-W_{3v}$	9.02	8.42	8.38	7.70

point sample involving Γ , X , L , and W leads to a band structure which is stable to about 0.1 eV. That is to say, the band structure should not change by more than about 0.1 eV with the inclusion of additional sampling points.

Using the four-point sample just mentioned, SC-OPW solutions were obtained for cubic ZnS, ZnSe, CdS, and CdSe using 229 OPWs at Γ (and a comparable number of OPWs at X , L , and W). The calculated energy levels are shown for reference in Table IV. The convergence properties of these solutions both as a function of the number of OPWs used per point and the

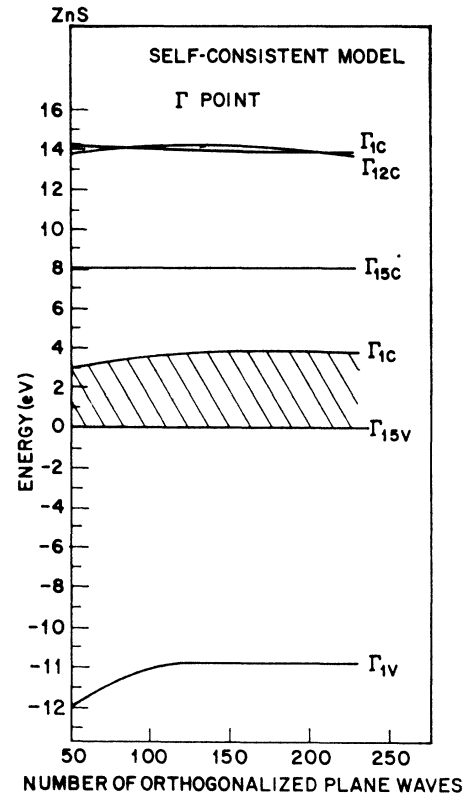


Fig. 2. Convergence study of SC-OPW energy levels at Γ point in cubic ZnS.

number of sample points used were carefully checked in all cases.

For purposes of comparison with Fig. 1, the convergence properties of the SC-OPW solutions for cubic ZnS are shown in Fig. 2. In going from 181 to 229 OPWs, the SC-OPW Γ_{1v} , Γ_{1c} , and Γ_{15c} levels change by less than 0.005 eV, while the SC-OPW Γ_{15v} level changes by about 0.02 eV on an absolute scale. In Figs. 1 and 2, we have actually treated Γ_{15v} as a fixed reference level, and shown all changes with respect to this fixed reference. At 229 OPWs, the over-all convergence of our SC-OPW energy levels is probably within a few hundredths of an eV.

It is noteworthy that beyond a certain number of OPWs, the SC-OPW solutions are more rapidly convergent than the NSC-OPW solutions. This appears to be a consequence of the smoothing introduced by the self-consistent iteration.

The lattice constants used in the present calculations are listed in Table V. Since different sources sometimes quote slightly different values for the lattice constants, we decided to find out how much the band structure changed if the lattice constant was changed slightly. Accordingly, we carried out two sets of self-consistent calculations for ZnSe, using lattice constants which differed by 0.2%. This led to direct band gaps which differed by 0.08 eV. Thus, even if we have to contend

TABLE V. Lattice constants used in SC-OPW and NSC-OPW band calculations, and core-shift energies for the latter. The lattice constants are given in Angstrom units, and the core-shift energies in rydbergs.

Crystal	Lattice constant ^a	Zn or Cd core shift	S or Se core shift
Cubic ZnS	5.41	-1.746	-1.839
Cubic ZnSe	5.65	-1.628	-1.584
Cubic CdS	6.081 ^b	-1.572	-1.418
Cubic CdSe	5.839	-1.377	-1.289

^a J. C. Slater, *Quantum Theory of Molecules and Solids* (McGraw-Hill Book Co., New York, 1965), Vol. 2, pp. 339 and 342. The lattice constants for cubic CdS and CdSe were obtained by assuming that the volumes of their unit cells are exactly half as large as in wurtzite-type CdS and CdSe. The lattice constants for wurtzite-type CdS and CdSe are given in Slater, p. 339.

^b See also: M. Balkanski and J. des Cloiseaux, *J. Phys. Radium* 21, 825 (1960).

with lattice constants which are uncertain by about 0.2%, we know that the corresponding uncertainty in the band structure is only about 0.1 eV.

For the benefit of those who might wish to repeat the present set of NSC-OPW band calculations, we show in Table V the core-shift energies¹³ which arise in such calculations. These energies represent the sum of all the overlapping atomic potentials at the cation and anion lattice sites. These core-shift energies also represent the amounts by which the free-atom core-electron energy levels are shifted by the formation of a crystal, at least within the framework of the overlapping atomic potential model. Self-consistent iteration will usually cause the core energy levels to depart slightly from their starting values (as given by the overlapping atomic potential model). The outermost *d* electrons are particularly sensitive to charge redistributions produced by self-consistent iteration (see also Sec. V).

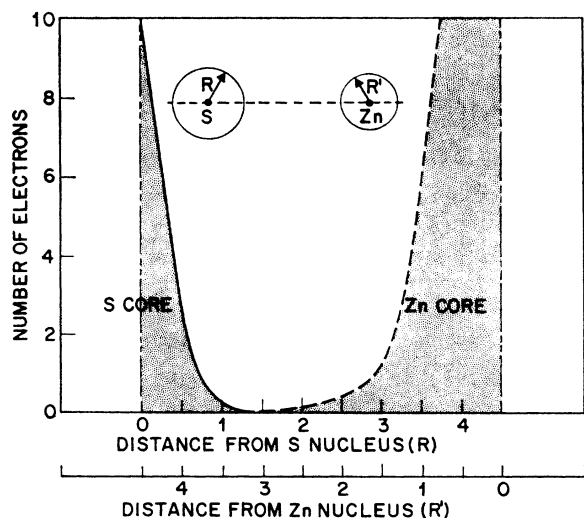


FIG. 3. Core-overlap study for cubic ZnS. The number of S core electrons lying outside a sphere of radius *R* centered at the S nucleus is indicated by the solid curve. The analogous curve for the Zn core electrons is shown dashed.

In the usual OPW formalism, it is assumed that there is negligible overlap between neighboring core-electron charge distributions. In order to see whether our calculations conformed to this assumption, we plotted the number of cation and anion core electrons lying outside spheres of varying radii surrounding the cation and anion lattice sites. Such a plot for ZnS is shown in Fig. 3. (The plots for ZnSe, CdS, and CdSe are similar.) If we draw cation- and anion-centered spheres through the point on the line connecting their centers where the Zn and S core-electron charge densities are equal, we find that only 0.05 electron lies outside these spheres. This result suggests that core overlap effects will have a negligible influence on the band structure. (We note in passing that the *3d* electrons in Zn and the *4d* electrons in Cd were treated as core electrons.)

For further details concerning the present set of SC-OPW band calculations, see Ref. 15.

III. COMPARISON OF VARIOUS THEORETICAL ENERGY-BAND MODELS

The results of NSC-OPW and SC-OPW band calculations for cubic ZnS, ZnSe, CdS, and CdSe, are listed in Tables VI-IX. Also shown in these tables are the results of ER-OPW band calculations (see Sec. IV for a further discussion of this information). In Tables VI and VII we also show, for purposes of comparison, the

TABLE VI. Comparison of various theoretical energy-level schemes for cubic ZnS.^a All entries are in eV.

Level	SC-OPW ^b	NSC-OPW ^b	ER-OPW ^b	ER-KKR ^c	Pseudo ^d calc (est)
Γ_{15c}	8.0	8.8	9.0	9.0	8.9
Γ_{1c}	3.8	4.3	3.7*	3.7*	3.7 (3.8)
Γ_{15v}	0.0	0.0	0.0	0.0	0.0
Zn <i>3d</i>	-14.1	-4.0	-5.0	-6.9	
X_{3c}	6.0	6.2	6.4	6.0	6.0
X_{1c}	5.0	5.9	5.6	5.7	5.2
X_{3v}	-1.6	-1.2	-1.1	-1.2	-1.5
X_{3v}	-3.9	-3.4	-3.3	-3.5	
$X_{3c}-X_{3v}$	7.6	7.4	7.5	7.5	7.5 (7.3)
$X_{1c}-X_{3v}$	6.6	7.1	6.7	7.2	6.7 (6.8)
$X_{3c}-X_{1c}$	1.0	0.3	0.8*	0.3	0.8 (0.5)
L_{3c}	8.6	9.3	9.4	9.3	8.7
L_{1c}	5.0	5.6	5.4	5.3	5.3
L_{3v}	-0.6	-0.4	-0.3	-0.6	-0.5
L_{1v}	-4.2	-3.5	-3.5	-3.7	
$L_{3c}-L_{3v}$	9.2	9.7	9.7	9.9	9.2 (9.5)
$L_{1c}-L_{3v}$	5.6	6.0	5.7*	5.9	5.8 (5.9)

^a Purely first-principles solutions are represented by the self-consistent and non-self-consistent OPW calculations (SC-OPW) and NSC-OPW. Empirically refined first-principles solutions are represented by ER-OPW and ER-KKR. For these solutions, entries that have been adjusted to experimental estimates are denoted by an asterisk. The energies calculated by the empirical pseudopotential method (PSEUDO) are listed in the column headed calc; the corresponding experimental estimates are shown in parentheses in the column headed est. Apart from the direct band gap, the various experimental estimates are uncertain by a few to several tenths of an eV.

^b Present work. SC-OPW and NSC-OPW are based on 229 OPWs at the zone center, while ER-OPW is based on 181 OPWs at the zone center. The present ER-OPW solution represents a slightly improved version of similar solutions published earlier (Ref. 3).

^c Based on the work of Eckelt, Madelung, and Treusch (Ref. 2).

^d Based on the work of Cohen and Bergstresser (Ref. 1). Improved pseudopotential solutions have recently been obtained for ZnS and ZnSe (M. L. Cohen, private communication).

results of ER-KKR⁵⁻⁷ and empirical pseudopotential (PSEUDO)² band calculations for ZnS and ZnSe.

Let us first address ourselves to the NSC-OPW and SC-OPW solutions, all of which were obtained using 229 OPWs at the zone center (and a comparable number of OPWs at other points in the zone). All of these solutions are well converged with respect to the number of OPWs used per point. In addition, the SC-OPW solutions are probably convergent to within about 0.1 to 0.2 eV with respect to the number of points sampled in the reduced zone.

As can be seen from these tables, the general consequence of self-consistent iteration is a reduction in the energy separation between valence and conduction bands. For example, the direct band gap $\Gamma_{1c}-\Gamma_{15r}$ is reduced by 0.3 eV in ZnSe; by 0.5 eV in ZnS; by 0.9 eV in CdSe; and by 1.5 eV in CdS. Similarly, the reduction in $\Gamma_{15c}-\Gamma_{15v}$ is 0.8 eV in ZnS; 0.9 eV in ZnSe; 1.5 eV in CdSe; and 1.9 eV in CdS. The reduction in energy separation between valence and conduction bands is usually smaller for crystals whose constituent atoms are nearly the same in atomic number or size (e.g., ZnSe and ZnS), than for crystals where this is not the case (e.g., CdSe and especially CdS).

On the other hand, the conduction-band splitting at $X(X_{3c}-X_{1c})$ becomes larger as one proceeds from NSC-OPW to SC-OPW solutions. These particular changes are smallest for ZnSe (0.2 eV), and somewhat larger for CdS (0.4 eV), CdSe (0.5 eV), and ZnS (0.6 eV).

Another striking change in going from NSC-OPW to SC-OPW is the broadening of the three uppermost valence bands. For example, in CdS, the width of the two highest valence bands actually doubles (cf. X_{5v} and L_{3v}), and the width of the third-highest valence band also increases considerably (cf. X_{3v} and L_{1v}).

To some extent, the change in the band structure produced by self-consistent iteration is the result of a

TABLE VII. Comparison of various theoretical energy-level schemes for cubic ZnSe. See the footnotes for Table VI for further details.

Level	SC-OPW	NSC-OPW	ER-OPW	ER-KKR	Pseudo calc (est)
Γ_{15c}	6.7	7.6	7.7	8.0	7.9
Γ_{1c}	2.9	3.2	2.8*	2.9*	2.9 (2.9)
Γ_{15v}	0.0	0.0	0.0	0.0	0.0
Zn 3d	-12.6	-5.3	-6.3	-7.1	
X_{3c}	4.5	5.1	5.4	5.1	5.4
X_{1c}	4.2	5.0	4.2	4.9	4.5
X_{5v}	-1.7	-1.3	-1.4	-1.6	-1.5
X_{3v}	-4.3	-3.7	-3.4	-4.0	
$X_{3c}-X_{5v}$	6.2	6.4	6.8	6.7	6.9 (7.2)
$X_{1c}-X_{5v}$	5.9	6.3	5.6	6.5	6.0 (6.4)
$X_{3c}-X_{1c}$	0.3	0.1	1.2*	0.2	0.9 (0.8)
L_{3c}	7.4	8.1	8.1	8.5	7.9
L_{1c}	3.8	4.3	4.5	4.3	4.5
L_{3v}	-0.6	-0.5	-0.4	-0.7	-0.5
L_{1v}	-4.4	-3.8	-3.7	-4.2	
$L_{3c}-L_{3v}$	8.0	8.6	8.5	9.2	8.4 (8.4)
$L_{1c}-L_{3v}$	4.4	4.8	4.9*	5.0	5.0 (5.0)

TABLE VIII. Comparison of various theoretical energy-level schemes for cubic CdS. See the footnotes for Table VI for further details.

Level	SC-OPW	NSC-OPW	ER-OPW
Γ_{15c}	7.6	9.5	9.8
Γ_{1c}	2.7	4.2	2.5*
Γ_{15v}	0.0	0.0	0.0
Cd 4d	-16.6	-4.2	-5.7
X_{3c}	5.7	7.0	7.2
X_{1c}	4.9	6.6	6.0
X_{5v}	-1.4	-0.7	-0.6
X_{3v}	-3.3	-2.2	-2.2
$X_{3c}-X_{5v}$	7.1	7.7	7.8
$X_{1c}-X_{5v}$	6.3	7.3	6.6
$X_{3c}-X_{1c}$	0.8	0.4	1.2*
L_{3c}	8.2	9.8	10.1
L_{1c}	4.3	6.0	5.4
L_{3v}	-0.6	-0.3	0.1
L_{1v}	-3.6	-2.3	-2.1
$L_{3c}-L_{3v}$	8.8	10.1	10.0
$L_{1c}-L_{3v}$	4.9	6.3	5.3*

redistribution of valence electrons (chemical bond formation). This charge redistribution is of considerable physical, chemical, and crystallographic interest; we hope to discuss this further in subsequent publications. For the present, we will concentrate on the changes in the energy-band structure associated with the passage from NSC-OPW to SC-OPW.

It is fairly evident that a valence-electron charge redistribution will lead to a change in the crystal Coulomb potential through Poisson's equation, and also to a change in the crystal exchange potential (recall that we are using Slater's free-electron exchange approximation). In the interest of completeness, we should mention that self-consistent iteration also leads to changes in the core-electron distribution, but these changes are usually quite negligible.

TABLE IX. Comparison of various theoretical energy-level schemes for cubic CdSe. See the footnotes for Table VI for further details.

Level	SC-OPW	NSC-OPW	ER-OPW
Γ_{15c}	6.6	8.1	8.3
Γ_{1c}	2.3	3.2	1.9*
Γ_{15v}	0.0	0.0	0.0
Cd 4d	-14.7	-5.2	-6.9
X_{3c}	4.7	5.8	5.9
X_{1c}	4.2	5.7	4.9
X_{5v}	-1.4	-0.8	-0.8
X_{3v}	-3.5	-2.6	-2.5
$X_{3c}-X_{5v}$	6.1	6.6	6.7
$X_{1c}-X_{5v}$	5.6	6.5	5.7
$X_{3c}-X_{1c}$	0.5	0.1	1.0*
L_{3c}	7.2	8.6	8.6
L_{1c}	3.7	4.8	4.3
L_{3v}	-0.5	-0.3	-0.1
L_{1v}	-3.6	-2.6	-2.5
$L_{3c}-L_{3v}$	7.7	8.9	8.7
$L_{1c}-L_{3v}$	4.2	5.1	4.4*

If the starting or trial crystal potential used in the NSC-OPW band calculations¹³ adhered as closely to the free-electron exchange approximation as the SC-OPW band calculations do, the difference between NSC-OPW and SC-OPW solutions would represent a true measure of the changes in the band structure produced by changes in the electronic charge distribution.

It is appropriate to recall, therefore, that the trial crystal potential used in the NSC-OPW band calculations has the form of a spatial superposition of overlapping atomic potentials. Each of these atomic potentials is represented in practice by a nonrelativistic self-consistent neutral-atom potential of the Hartree-Fock-Slater free-electron exchange variety.²⁶ In contrast to Ref. 26, the atomic exchange potentials used here are proportional to the cube root of the atomic charge density for all values of r . Since the atoms are chosen to be electrically neutral, the atomic Coulomb potentials approach zero at large values of r , and so do the atomic exchange potentials. In short, the crystal potential is represented by a spatial superposition of overlapping atomic potentials each of which approaches zero at large distances from its respective center.

While this representation has many attractive physical and mathematical features—this is why it was introduced in the first place¹³—the resulting crystal exchange potential does not have quite the form demanded by the free-electron exchange approximation. According to this representation (overlapping atomic potential model), the crystal exchange potential is expressed

$$V_{\text{exchange}}^{\text{crystal}}(\mathbf{r}) = -6 \sum_{\mathbf{d}} \sum_{\mathbf{f}} \left[\frac{3}{8\pi} \rho_{\mathbf{f}}^{\text{atom}}(\mathbf{r} - \mathbf{d} - \mathbf{f}) \right]^{1/3} \quad (1)$$

rather than

$$V_{\text{exchange}}^{\text{crystal}}(\mathbf{r}) = -6 \left[\frac{3}{8\pi} \sum_{\mathbf{d}} \sum_{\mathbf{f}} \rho_{\mathbf{f}}^{\text{atom}}(\mathbf{r} - \mathbf{d} - \mathbf{f}) \right]^{1/3}, \quad (2)$$

where the sums are taken over all direct lattice vectors \mathbf{d} and basis vectors \mathbf{f} , and where V is expressed in rydbergs.

Although the differences between Eqs. (1) and (2) are estimated to be rather small for the crystals under study, they are sufficiently large to account for a non-trivial fraction of the differences between NSC-OPW and SC-OPW energy-level schemes so apparent in Tables VI–IX. In short, the differences in Tables VI–IX are due only in part to changes in the valence-electron distribution induced by self-consistent iteration; they are also due in part to the approximate construction of the crystal exchange potential in the NSC-OPW calculations.

It is, of course, possible to calculate the difference between Eqs. (1) and (2), and to use this difference as an improvement in the NSC-OPW calculations. We have

²⁶ F. Herman and S. Skillman, *Atomic Structure Calculations* (Prentice-Hall, Inc., Englewood Cliffs, N. J., 1963).

not followed this course for two quite separate reasons: If our ultimate objective is a SC-OPW solution, then the NSC-OPW calculation provides a convenient starting point, and the difference between Eqs. (1) and (2) is automatically taken care of on the first iteration. On the other hand, if our ultimate objective is an ER-OPW solution, then the difference between Eqs. (1) and (2) can be absorbed in the empirical correction. In either case, it is not *essential* to ascertain the actual difference between Eqs. (1) and (2).

It is clear from Tables VI–IX that the various theoretical energy-band models are quite similar qualitatively and semiquantitatively, but that there are often appreciable quantitative differences from solution to solution. The empirical pseudopotential solutions of Cohen and Bergstresser² (PSEUDO) were adjusted to the experimental values for the direct band gaps, and to rough estimates of other key interband transition energies. While the direct band gaps are usually known to within about 0.1 eV, the other estimates are uncertain by about 0.5 eV. The ER-KKR solutions of Eckelt, Madelung, and Treusch^{5–7} are based on first-principles calculations supplemented by small empirical corrections, the spirit here being similar to that of our own ER-OPW solutions.^{8–10} In the case of the ER-KKR solutions, the empirical correction amounted to shifting the constant part of the muffin-tin potential relative to the spherical atomic potential parts. The shift was designed to bring calculated band gaps into agreement with experiment. Since this type of empirical correction is only one of several possible types,^{8–10} there is no guarantee that the values of the other interband transition energies are actually brought closer to experiment by this correction. It is also not clear how drastically the first-principles KKR solutions would be altered by self-consistent iteration.

IV. EMPIRICALLY REFINED OPW BAND CALCULATIONS

In Tables VI–IX we also show the results of ER-OPW band calculations for cubic ZnS, ZnSe, CdS, and CdSe. The starting point of these calculations is a set of NSC-OPW solutions based on 181 OPWs at the zone center. (If we had used a similar set of solutions based on 229 OPWs at the zone center as the point of departure, the outcome would have been the same, within a few tenths of an eV.) In order to improve the agreement between our first-principles solutions (NSC-OPW) and experiment, we make use of a three-parameter empirical correction scheme which we have employed with considerable success in earlier studies of sphalerite-type crystals.^{8–10} Two of the empirical parameters (cation and anion core shifts) are used to modify the effective crystal potential in the ion core regions, and the third [symmetric component of $v(111)$] to raise or lower the potential in the interstitial region relative to the ion core regions. The three parameters are so chosen

that the calculated values of three key interband transition energies agree with their experimental counterparts (or with estimates based on our own analysis of experimental reflectivity spectra).

Our empirical adjustment scheme is considerably more flexible and realistic than that used in the ER-KKR calculations mentioned above. The KKR adjustment scheme is equivalent to ignoring the symmetric component of $v(111)$, and setting the anion and cation core shifts equal to one another. Our three-parameter scheme allows for independent adjustments of the anion and cation core shifts, and for an increase or decrease in the magnitude of the potential "arches" in the interstitial region.

We generally carry out our empirical adjustments by assigning suitable values to the band gap at Γ , $\Gamma_{1c} - \Gamma_{15v}$; the band gap at L , $L_{1c} - L_{3v}$; and the band gap at X , $X_{1c} - X_{5v}$. The first of these quantities is usually a well-known experimental quantity; the second can be estimated from the location of the first reflectivity peak (within a few tenths of an eV); and the third can be estimated from the location of the second (main) reflectivity peak (also within a few tenths of an eV). In our treatment, $L_{1c} - L_{3v}$ is set equal to the energy of the first reflectivity peak (though it could equally well be set 0.1 or 0.2 eV lower than this), and $X_{1c} - X_{5v}$ is set a few to several tenths of an eV less than the energy of the second (main) reflectivity peak. In choosing a value for $X_{1c} - X_{5v}$, an attempt is made to obtain a reasonable value for $X_{3c} - X_{1c}$, as well. Since it is difficult to determine the value of $X_{3c} - X_{1c}$ from an inspection of the experimental reflectivity curve, we have adopted certain estimates, which we arrive at as follows.

In the isoelectronic sequence Ge-GaAs-ZnSe, it is reasonable to assume that $X_{3c} - X_{1c}$ is a linear function of the "antisymmetric potential." Since $X_{3c} - X_{1c}$ is 0 in Ge, and 0.6 eV in GaAs, we adopt a value of 1.2 eV for $X_{3c} - X_{1c}$ in ZnSe. Next, let us consider the isoelectronic sequence GeSi-GaP-ZnS. Knowing that $X_{3c} - X_{1c}$ is 0.2 eV in GaP, and assuming that this X splitting changes by 0.6 eV as one moves from the III-V compound to the IV-IV or II-VI compound, we obtain an X splitting of -0.4 eV for GeSi, and 0.8 eV for ZnS. The value thus obtained for ZnS is a reasonable one, and we will adopt it. (Digression: If the Ge and Si atoms are interchanged in the unit cell, the symmetry labels $X_{3c} - X_{1c}$ are also interchanged.) If this is done, we obtain a value of $+0.4$ eV for $X_{3c} - X_{1c}$ in SiGe. By an extension of the same argument, we would obtain a value of $+1.0$ eV for $X_{3c} - X_{1c}$ for AsAl (AlAs), an estimate which we also consider reasonable.

Before turning to the isoelectronic sequence SnGe-InAs-CdSe, let us consider the closely related sequence GeSn-GaSb-ZnTe. According to some of our earlier studies¹⁰ of GaSb and ZnTe, $X_{3c} - X_{1c}$ is 0.2 eV in GaSb and 0.6 eV in ZnTe. Assuming that this X splitting

changes by 0.4 eV from member to member in this sequence (and also in the SnGe-InAs-CdSe sequence), we find an X splitting of -0.2 eV in GeSn, or of $+0.2$ eV in SnGe; an X splitting of 0.6 eV in InAs, and an X splitting of 1.0 eV in CdSe (which we adopt). By similar arguments we obtain a value of 1.2 eV for CdS.

In Tables VI-IX the ER-OPW energy levels that were adjusted to experiment (or to reasonable estimates) are marked with an asterisk. The remaining values were obtained from the original solutions by taking the empirical corrections into account.

V. OPTICAL SPECTRUM CALCULATIONS

If accurate experimental values were available for all the interband transition energies listed in Tables VI-IX, it would be a simple matter to decide which theoretical model was in best over-all agreement with experiment. Unfortunately, only the band gaps (optical thresholds) are accurately known (say within 0.1 eV). It is possible to obtain rough estimates of certain other interband transition energies by calculating the optical spectrum (actually ϵ_2) and comparing this with its experimental counterpart.

However, available experimental reflectivity spectra are often of uncertain accuracy, and the derived experimental ϵ_2 spectra are correspondingly uncertain. In some cases the experimental reflectivity spectra are available but the derived ϵ_2 spectra are not, so that one has to contend with the possible differences between these two types of spectra. Apart from such considerations, one must bear in mind that the optical spectrum is a weighted sum over all possible direct interband transitions; each transition is weighed by its oscillator strength. Since it is not possible to calculate the oscillator strengths with a high degree of accuracy, there will often be serious discrepancies in magnitude and shape between theoretical and experimental optical spectra. But even if such discrepancies are discounted, and one compares only prominent spectral features, such as peaks and shoulders, there are still many aspects of the underlying energy band model that are not really tested by such comparisons. In particular, one cannot establish the values of interband transition energies associated with regions which do not contribute importantly to the optical spectrum, and one cannot determine the relative positions of energy levels at different points in the zone.

In spite of these shortcomings, it is still instructive to carry out optical spectrum calculations, and to compare the outcome with experiment. For the moment, let us focus our attention on the SC-OPW energy level schemes listed in Tables VI-IX. The calculated energy levels at the sample points (Γ , X , L , and W) are shown in Figs. 5-8 as heavy dots. (The reduced zone is displayed for convenience in Fig. 4.) We have determined the band structure in the remainder of the zone by fitting a pseudopotential-type interpolation scheme to the cal-

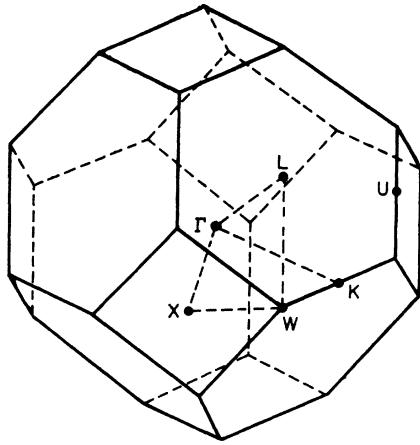


FIG. 4. Reduced zone for sphalerite-type crystals.

culated energy levels at the sample points. The solid lines in Figs. 5-8 were drawn in with the aid of this interpolation scheme. (A detailed account of this scheme is presently being prepared for publication by Euwema, Stukel, Collins, DeWitt, and Shankland.) Also shown in these figures is the location of the 3*d* band in Zn and ZnSe, and the 4*d* band in CdS and CdSe.

Using this interpolation scheme, the band energies, band-energy gradients, and optical transition matrix elements at each of 155 coarse mesh points in the irreducible sector (1/48th) of the reduced zone were evaluated. A fine mesh consisting of 512 points was then centered at each coarse-mesh point. The band energies

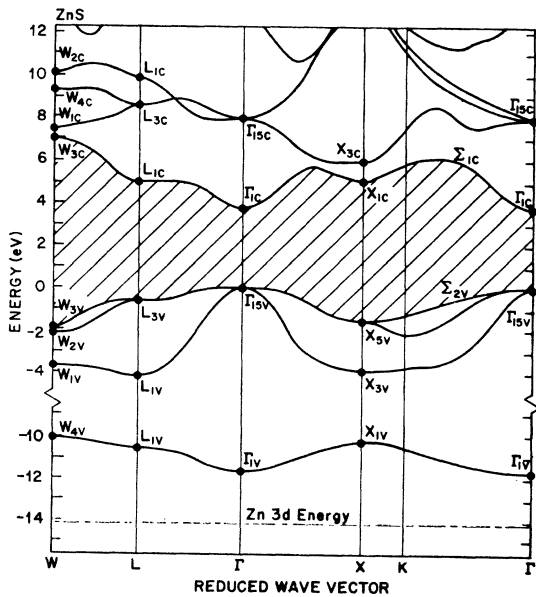


FIG. 5. SC-OPW energy-band structure of cubic ZnS. The solid dots denote SC-OPW energy levels. The solid lines were obtained by fitting a pseudopotential-type interpolation scheme to the SC-OPW energy levels.

at each of the fine mesh points were calculated from a knowledge of the band energies and band-energy gradients at the coarse-mesh points. The optical transition matrix elements at the coarse-mesh points were used for the associated fine-mesh points. The optical spectrum (ϵ_2) was then calculated by summing over all interband transitions at each of the 512×155 fine-mesh points. This process was repeated several times for each crystal

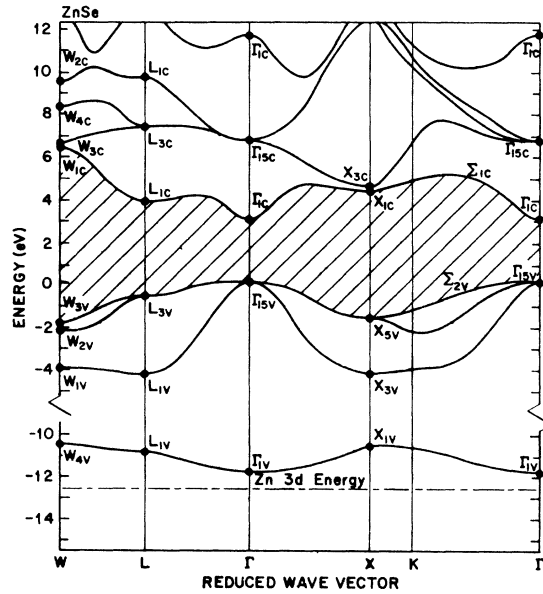


FIG. 6. SC-OPW energy-band structure of cubic ZnSe. For further details, see the caption for Fig. 5.

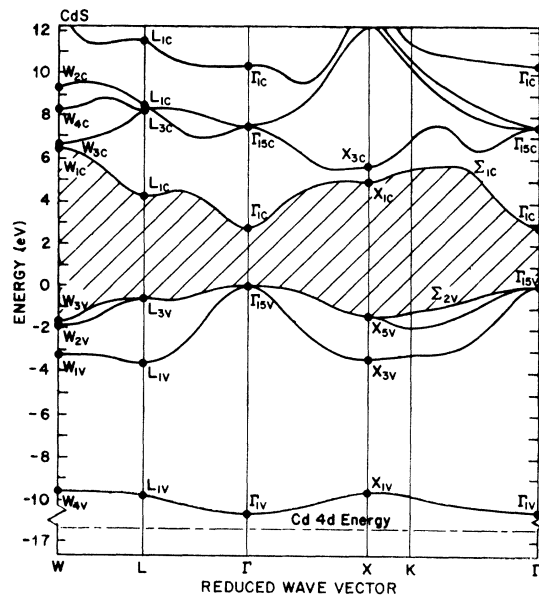


FIG. 7. SC-OPW energy-band structure of cubic CdS. For further details, see the caption for Fig. 5.

Experimental ϵ_2 curves for ZnS,^{27,28} ZnSe,²⁹ and CdS³⁰ are compared with the theoretical ϵ_2 curves in Figs. 9–11.

Since the calculation of optical transition probabilities is quite approximate—pseudopotential-type wave functions are used and electron-hole interactions are ignored in the present analysis—it is not surprising that there are significant differences in the detailed shapes of the theoretical and experimental optical spectra. The principal information to be obtained from Figs. 9–11 is the relative location of corresponding peaks. In addition to the experimental spectra displayed in these figures, one can turn to Pollak's extensive compilation of experimental information for cubic ZnS, ZnSe, and CdS,³¹ and to the experimental results of Ludeke and Paul^{32–34} for cubic ZnSe.

In the case of cubic ZnS (cf. Fig. 9), there is reasonable agreement between the three principal experimental and theoretical peaks. The first of these, at about 5.7 eV, is produced by $L_{3v} \rightarrow L_{1c}$ and related transitions. The second (main) peak at about 7.0 eV is produced by $\Sigma_{2v} \rightarrow \Sigma_{1c}$ and related transitions over a significant fraction of the reduced zone. The third peak at about 9.6 eV is produced by $L_{3v} \rightarrow L_{3c}$ and related transitions. The good agreement between theory and experiment confirms that $L_{1c}-L_{3v}$ and $L_{3c}-L_{3v}$ are given correctly by SC-OPW to within a few tenths of an eV. Since the leading edge of the second (main) peak is determined by $X_{1c}-X_{5v}$, and since the second peak "moves" with $\Sigma_{1c}-\Sigma_{2v}$, the theoretical (SC-OPW) value for $X_{1c}-X_{5v}$ is consistent with experiment to within a few tenths of an eV. It is not really possible to determine $X_{3c}-X_{5v}$ or $\Gamma_{15c}-\Gamma_{15v}$ with any degree of confidence from Fig. 9. In any event, the SC-OPW energy-band model for cubic ZnS leads to an optical spectrum which is in satisfactory agreement with the experimental spectrum over an extended range.

In the case of ZnSe (cf. Fig. 10), there is again good agreement between theory and experiment so far as the first peak at about 4.7 eV is concerned, but the second and third theoretical peaks (at 6.0 and 8.0 eV) lie about 0.4 eV below their experimental counterparts.³¹ In the case of CdS (cf. Fig. 11), the experimental spectrum is of rather poor quality (because of poor crystal samples), but even allowing for this, the situation is similar to that

²⁷ M. Balkanski and Y. Petroff, in *Proceedings of the International Conference on the Physics of Semiconductors, Paris, 1964* (Dunod Cie., Paris, 1964), p. 245. Improved experimental reflectivity and ϵ_2 spectra for ZnSe and other II-VI compounds have recently been obtained by these authors. Their new results will be published shortly.

²⁸ J. S. Baars, in Ref. 1, p. 631.

²⁹ M. Aven, D. Marple, and B. Segall, *J. Appl. Phys. Suppl.* 32, 226 (1961).

³⁰ M. Cardona, M. Weinstein, and G. A. Wolff, *Phys. Rev.* 140, A633 (1965).

³¹ F. H. Pollak, in Ref. 1, p. 552.

³² R. Ludeke and W. Paul, in Ref. 1, p. 123.

³³ R. Ludeke, Technical Report No. HP-22, Division of Engineering and Applied Physics, Harvard University, 1968 (unpublished).

³⁴ R. Ludeke and W. Paul, *Phys. Status Solid* 23, 413 (1967).

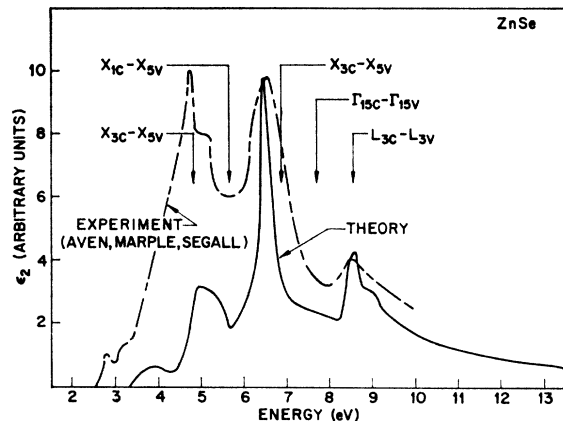


FIG. 13. Comparison of theoretical (ER-OPW) and experimental ϵ_2 curves for cubic ZnSe.

for ZnSe: The first theoretical peak (at 5.3 eV) is in reasonable agreement with experiment, but the second and third theoretical peaks (at 6.6 and 8.6 eV) appear to lie somewhat lower than their experimental counterparts. In CdSe, the first theoretical peak at about 4.7 eV is in reasonable agreement with the spin-orbit split doublet observed optically^{32–34} at 4.30 and 4.56 eV (room-temperature values). The second theoretical peak at about 5.7 eV is somewhat lower than its experimental counterpart, which occurs at 6.34 eV.^{32–34}

We have repeated the optical spectrum calculations for cubic ZnSe and CdSe using our ER-OPW solutions as the underlying energy-band models. The theoretical results are shown in Figs. 13 and 14. Since the ER-OPW energy-band models for these crystals were deliberately chosen to yield optical spectra which agree with experiment, it is hardly surprising that they do. Of course, the agreement between theoretical and optical spectra provides a check on some features of the energy-band structure, but does not resolve such questions as: What is the energy separation between X_{3c} and X_{1c} ?; between X_{1c} and Γ_{1c} ?; between L_{1c} and Γ_{1c} ?; between Γ_{15c} and Γ_{15v} ?

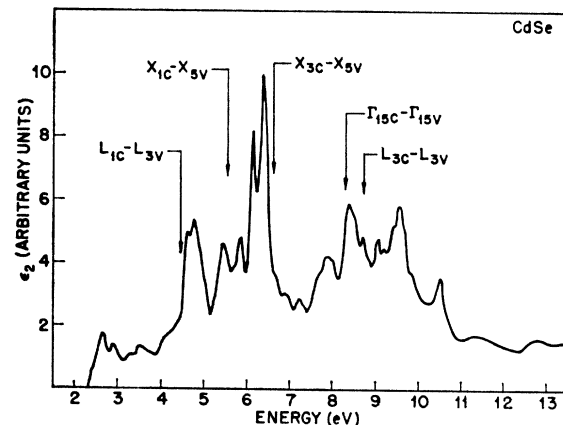


FIG. 14. Theoretical curve ϵ_2 for cubic CdSe, based on ER-OPW model.

We have not repeated the optical spectrum calculations for cubic ZnS or CdS using our ER-OPW solutions for two quite different reasons. In the case of ZnS, our ER-OPW solution is so close to our SC-OPW solution that both can be expected to yield essentially the same optical spectrum (and hence to agree with experiment). In the case of CdS, we did not feel it was worthwhile to recalculate the optical spectrum in view of the inferior quality of the experimental spectrum. However, we believe that the theoretical spectrum based on ER-OPW would be in better agreement with experiment than that based on SC-OPW.

To the extent that the ER-OPW solutions are closer to experiment than the SC-OPW and NSC-OPW solutions, a comparison of these three sets of solutions can be used to gauge the relative merits of the SC-OPW and NSC-OPW results.

Finally, a word is in order concerning the location of the $3d$ bands in ZnS and ZnSe, and the $4d$ bands in CdS and CdSe. The experimental reflectivity spectra of ZnS, ZnSe, CdS, and CdSe show high-energy peaks³¹ between 10.5 and 14.5 eV which have usually been attributed to transitions from the d bands in these materials to the conduction bands. This interpretation is clearly speculative, since these reflectivity peaks could equally well be associated with transitions from the lowest valence band (or even the higher valence bands) to the conduction bands. However, if we go along with the d -band interpretation, and pick for the final states the energy range in the conduction band having the highest density of states, we find that the d -band locations given by the ER-KKR,⁵⁻⁷ ER-OPW, and NSC-OPW energy-band models are in reasonable accord with experiment, while those given by the SC-OPW models are invariably too low. The first three types of band models usually place the d bands between the lowest and second lowest valence bands, while the SC-OPW models place the d bands somewhat below the lowest valence band (cf. Figs. 9-12). We are continuing to study the question of the d -band locations.

[In going from the NSC-OPW to the SC-OPW solutions, the d bands are found (by the Aerospace Research Laboratories group) to move downward in energy by several eV. This downward shift is associated with a redistribution of valence electron charge. In order to check this point, the Lockheed group calculated the band structure of ZnSe using Zn^+ and Se^- ions rather than neutral Zn and Se atoms (again within the framework of the overlapping atomic potential model). In going from Zn^0Se^0 to Zn^+Se^- (NSC-OPW), the Zn $3d$ band moves downward in energy by 4.3 eV, and the separation between valence and conduction bands is reduced by 0.7 to 1.7 eV. While both of these trends are in the same direction as those found by the Aerospace Research Laboratories group (in going from NSC-OPW to SC-OPW), the Lockheed group believes that the self-consistent charge transfer from Zn to Se should be of the order of $\frac{1}{3}$ of an electron charge, so that the Zn

$3d$ band should shift downward by only 1-1.5 eV, and the valence and conduction bands should approach each other by only 0.2-0.6 eV. It is not clear at present why the downward shifts in the d bands found by the Aerospace Research Laboratories group are so much larger.]

VI. CONCLUDING REMARKS

Both the SC-OPW and the NSC-OPW band calculations lead to energy-band schemes which are in qualitative and semiquantitative agreement with experiment. Considering the many simplifying assumptions inherent in these calculations, it is most gratifying that our first-principles results agree with experiment as well as they do. It is encouraging to find that some of the essential features of the calculated band structure and optical spectrum agree with experiment to within a few tenths of an eV. Some key features, such as the band gap and the first reflectivity peak, are often in better agreement with experiment for the SC-OPW solutions, while other important features, such as the second (main) and third reflectivity peaks, are usually in better agreement with experiment for the NSC-OPW solutions. As we have shown, the NSC-OPW solutions can be readily improved by the introduction of carefully chosen empirical corrections. The SC-OPW solutions can be similarly improved. In practice, the empirical corrections required to bring theory and experiment into agreement are quite small.

From the standpoint of physical rigor, the SC-OPW solutions are clearly superior to the NSC-OPW solutions. It must be emphasized that the comparison between the SC-OPW energy level scheme and experiment is physically more significant than that between the NSC-OPW scheme and experiment. The former comparison also provides a more incisive test of Slater's free-electron exchange approximation than does the latter. Our work provides some idea of the changes in the band structure of II-VI crystals that are produced by self-consistent iteration.

It is clear from our results that the treatment of exchange effects in crystals will have to be improved considerably before first-principles band calculations can be expected to agree with experiment to better than a few tenths of an eV over a wide energy range. It will also be necessary to carry out such calculations within a fully relativistic framework, and to take correlation effects into account more explicitly. As first-principles band calculations continue to improve, we expect to obtain not only better energy-level schemes, but better sets of crystal wave functions and better electronic charge distributions. In all of these developments, we expect to see self-consistent solutions come more and more into their own.

ACKNOWLEDGMENT

The authors are grateful to Dr. John P. Van Dyke for helpful comments concerning the manuscript.

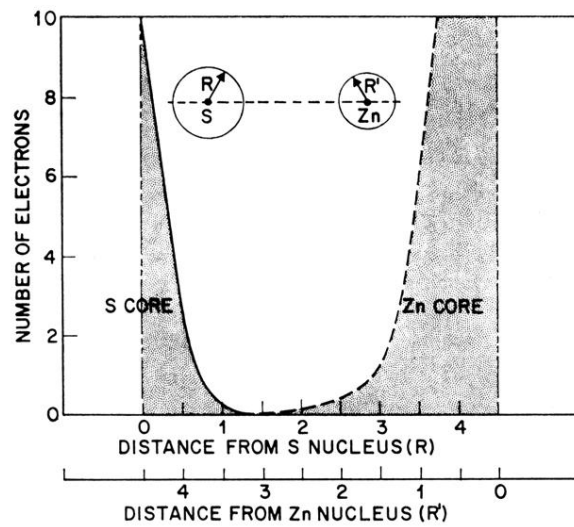


FIG. 3. Core-overlap study for cubic ZnS. The number of S core electrons lying outside a sphere of radius R centered at the S nucleus is indicated by the solid curve. The analogous curve for the Zn core electrons is shown dashed.